

The Binding Mode of Progesterone to Its Receptor Deduced from Molecular Dynamics Simulations

Tiziana Mordasini,^[a] Alessandro Curioni,^[a] Roberta Bursi,^[b] and Wanda Andreoni^{*[a]}

An unambiguous understanding of the binding mode of human progesterone to its receptor still eludes experimental search. According to the X-ray structure of the ligand-binding domain, only one (O3) of the two keto groups at the ligand ends (O3 and O20) should play a role. This result is in conflict with chemical intuition and the results of site-directed mutagenesis experiments. Herein, we report classical molecular dynamics simulations that reveal the dynamic nature of the binding in solution, elucidate the

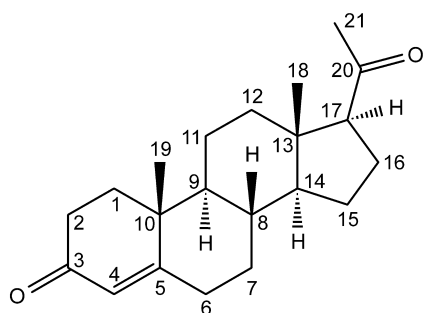
reasons why X-ray studies failed to determine the role of O20, and clarify the effects of the mutations. The predictive power of the force field is ensured by the consistent introduction of a first-principles representation of the ligand.

KEYWORDS:

bioorganic chemistry · density functional calculations · hormones · molecular dynamics · receptors

Introduction

Progesterone, “the hormone of pregnancy”, is a natural reference compound for the design of drugs with application in hormone-replacement therapy, oral contraception, and gynecological disorders. Controlling, activating, or blocking the action of the hormone progesterone amounts to modifying its binding with its receptor. Current knowledge of the ligand–receptor interaction at the molecular level mainly relies on the 1.8-Å X-ray structure^[1] of the ligand-binding domain (LBD) of the human-progesterone–receptor complex and, more indirectly, on the results of site-directed mutageneses^[2] and analogies with the other nuclear receptors.^[3, 4] Progesterone (Scheme 1) is a small



Scheme 1. The structure of progesterone.

hydrophobic molecule with a polar functional group at each end (O3 and O20 carbonyl groups); both groups are expected to interact with the receptor, in particular by hydrogen bonding. However, the X-ray structure^[1] revealed such an interaction only at the O3 end, for which a detailed picture emerged. The O20 end, on the contrary, did not appear to be directly involved in the binding. The overall refinement of the structure was good, as

suggested by the small difference between the values of the R (0.190) and the R_{free} factors (0.228).^[5]

To investigate the ligand–receptor binding with a different approach and to shed light on this puzzle, we performed molecular dynamics (MD) simulations in explicit solvent. Part of the simulations were specifically aimed at unraveling the role of water molecules. In this way, we attempt to understand to what extent the results of the crystallographic structure elucidation are representative of the receptor in vivo.

We chose classical MD as the simulation method. The entire system consists of more than 10 000 atoms, which precludes the application of a quantum-mechanical approach. Even a hybrid quantum–classical (QM/MM)^[6] approach is currently unaffordable given the time required for these simulations.^[7] A conventional force field designed to represent the dynamics of proteins in aqueous solution does not necessarily provide a reliable representation of the ligand, which requires special care in this case. O3 is a stronger hydrogen-bond acceptor than O20 because of the higher basicity and lower steric hindrance of O3.^[8] The parametrization adopted in most force fields correctly accounts for the difference in steric hindrance but does not distinguish between a conjugated keto group and an aliphatic one, and thus misses the difference in the chemical properties of such groups. In other cases, such as that of the estrogen–re-

[a] Dr. W. Andreoni, Dr. T. Mordasini, Dr. A. Curioni
IBM Research
Zurich Research Laboratory
8803 Rüschlikon (Switzerland)
Fax: (+41) 1724-8962
E-mail: and@zurich.ibm.com

[b] Dr. R. Bursi
Molecular Design & Informatics Department
N. V. Organon, 5340 BH Oss (The Netherlands)

ceptor complex, description of the binding mode is less problematic for classical MD simulations^[9] because the two interacting ends contain functional groups for which specific parametrization is available. Another issue regarding the O20 end is that the probability of this O atom forming H bonds is sensitive to the torsional potential of the acetyl group. This also needs careful description. Therefore, we used the GROMOS96 force field,^[10, 11] which has been demonstrated to be reliable for proteins, and modified its parameters for the ligand (relevant effective charges for the conjugated keto group and torsional potential at the O20 end) on the basis of accurate quantum-mechanical calculations performed within the framework of density functional theory (DFT).^[12] This procedure should guarantee unbiased predictions of the propensity of the ligand to form hydrogen bonds and the specificity of its interactions. Finally, we used a recently developed QM/MM method^[6] to explore key features of the bonding.

The results of these simulations turned out to be in agreement with the X-ray structure for the binding mode at the O3 end^[1] and also revealed the dynamic nature of the water molecules that interact with the ligand. Moreover, we were able to identify the binding mode at the O20 end and provide insight into why crystallographic work missed this binding. Finally, additional simulations of the mutant Cys891Ser could help rationalize the loss of binding activity observed experimentally in site-directed mutagenesis studies.^[2]

Results and Discussion

Scheme 1 shows the structure of the progesterone molecule. The crystallographic structure of the progesterone receptor LBD at the O3 and the O20 end is shown in Figure 1a and 1b, respectively. The complex crystallizes in the form of a dimer with a small dimer interface (705 \AA^2)^[1] and is a monomer in aqueous solution.^[13] Therefore, we modeled the monomeric ligand–protein complex in aqueous solution and studied its dynamics at room temperature by using the X-ray structure as the initial configuration.

The parametrization we adopted is that of the GROMOS96 force field,^[10] into which we introduced modifications both for the effective atomic charges of the conjugated keto group at the O3 end of the ligand and for the representation of the torsional potential of the acetyl group at C17 (Scheme 1). A force field developed for static docking models (see for example, MMFF^[14]) would have provided a good representation of the ligand but would not have been suitable for simulation of the protein dynamics in explicit water. We determined the new effective charges by adjusting their values to reproduce the electrostatic potential of the progesterone obtained from DFT calculations. In the fitting procedure, the charge values were restrained to the GROMOS96 range.^[10] This restraint was important to maintain consistency of the global parametrization, which was originally obtained by the simultaneous optimization of all effective charges as well as the description of van der Waals interactions. Lack of consistency would otherwise corrupt the reliability of the results. As can be seen in Scheme 2, the changes were significant: the charge is no longer localized exclusively and

equally on O3 and C3, it distributes itself over all the atoms of the conjugated keto group and, importantly, the absolute values of the charges increased compared to the original GROMOS values. We derived the new parametrization of the torsional potential of the acetyl group at C17 so as to reproduce as closely as possible the DFT total energy as a function of the torsional angle. In contrast to previous attempts of this kind,^[15] our fitting takes into account the entire ligand as well as the new prescription for the effective charges, which once again guarantees internal consistency and model transferability. Figure 2 compares the GROMOS96 energy profile and our corrected one. The positions of the energy minima obtained with the standard GROMOS96 parametrization differ from the ab initio values; the lowest minimum is shifted by about 10 degrees. Both the energy minima and the relative barriers decrease significantly when the GROMOS96 model is adjusted as described, for example, the main barrier decreases by 13 kJ mol^{-1} .

Figure 3 shows the Debye–Waller or B factors calculated for both the protein and the ligand by averaging the atomic trajectories (approximately 1 ns) and compares them with experimental data.^[1] The overall good agreement is comforting, although we are aware that Debye–Waller factors are not a critical test of the force field.^[16]

To validate our computational scheme, we first consider the environment of the O3 end of the hormone, for which a clear picture emerges from experiment.^[1] In the X-ray structure (Figure 1a), O3 interacts with Arg766 and Gln725 through hydrogen bonds, and two water molecules help stabilize the structure, one by connecting these two amino acids and the other by bridging Gln725 to the carbonyl groups of Ile699 and Phe778. The residues have greater flexibility in the simulated system in solution (Figure 1c) than in the crystallographic structure. Residues switch from one type of orientational conformation to the other, which gives rise to different sets of configurations of the entire complex. To allow a better comparison of calculated values with X-ray data, we report separate averages for these different configuration sets. Most of the time, the residues are in the rotational states corresponding to those in the crystal structure. The calculated net of hydrogen bonds and all individual distances are in close agreement with experimental observation. However, whenever the residues switch to different rotational states, the receptor loosens its specific interaction with the ligand and prefers to interact with the solvent. In agreement with experiment, our simulations reveal that there is always a water molecule at each of the two bridging positions between the residues that interact dynamically through H bonds. Moreover, the identity of these water molecules changes over time; a continuous dynamic exchange with water molecules from the bulk solvent takes place. Over 2 ns, the residence time of a water molecule varies between 300 and 700 ps.

This same type of simulation, when carried out with GROMOS standard effective charges, provided a picture significantly different from ours, as shown in Scheme 2. In fact, in contrast to experimental evidence, the weaker GROMOS charges and their stronger localization result in a partial disruption of the hydrogen-bond network, in favor of interactions with the bulk

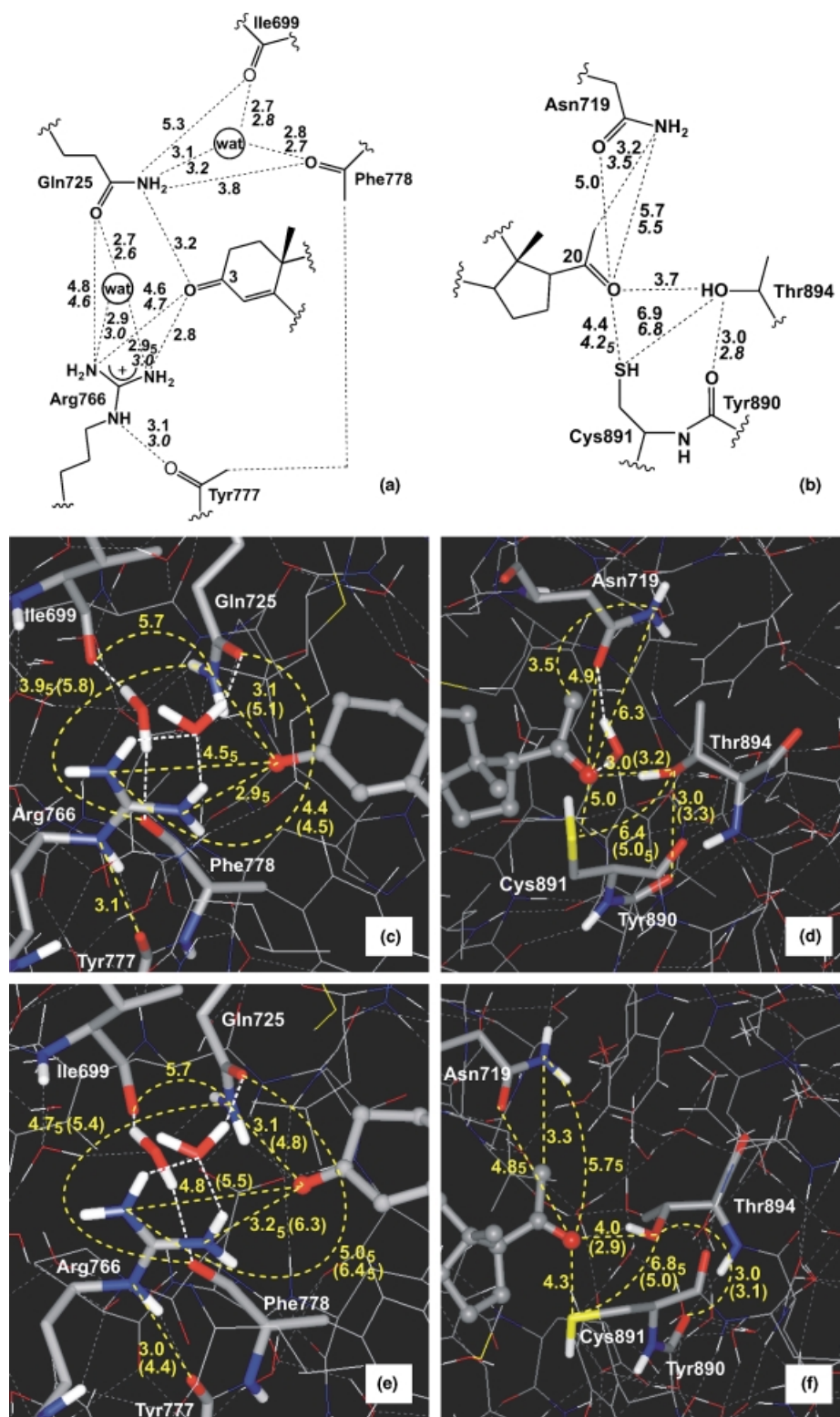
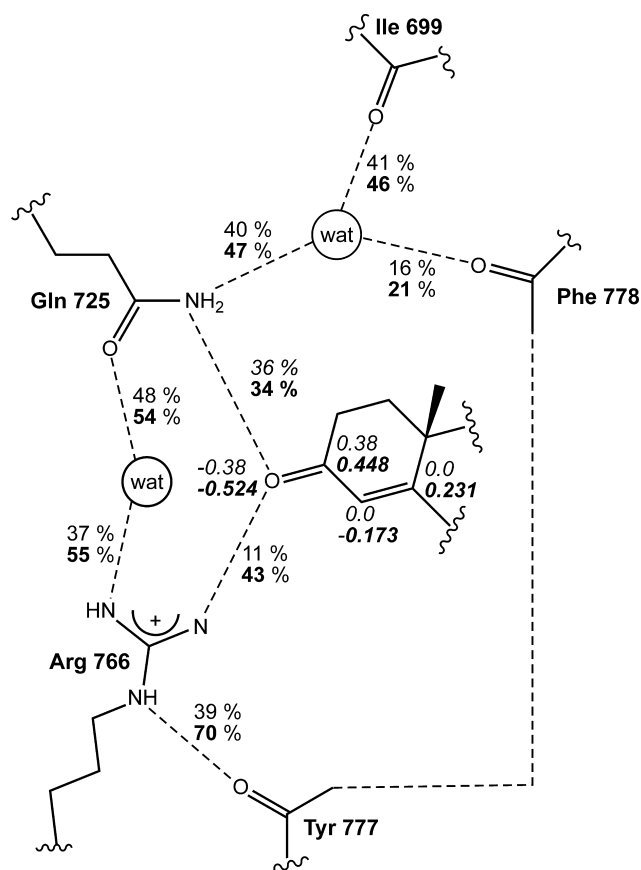


Figure 1. Scheme of the ligand – protein interactions around the O3 and O20 ends of progesterone. (a) and (b) refer to the X-ray structure of Ref. [1] available from the Protein Data Bank (1a28). Distances are given in Å. Some minor discrepancies exist with respect to the previously published values. The two different values given refer to the distances in the two chains of the dimer; if these are the same, only one value is given. (c) and (d) are representative configurations from simulation in aqueous solution. (e) and (f) are representative configurations from additional simulations in aqueous solution in which one water molecule around the O20 end was constrained to reside outside the binding pocket. Note that the water molecule interacting with the amino group of Gln725 is H bonded to both Phe778 and Ile699 (see text). The H bond with Ile699 was not apparent from Ref. [1] and has been omitted in the subsequent literature. In the MD runs, the residues are free to rotate, which gives rise to different ensembles of conformations. Whenever more than one set of conformations is sampled, we report more than one value for the distances, each being the average over the respective residence times. The values in parentheses in (c–f) refer to the set of conformations that differ from that in the crystallographic structure in (a) and (b) because of these rotations. The most important changes in the pattern of distances in (c) and (d) that result from the replacement of Cys891 with Ser concern Thr894, which constantly points towards O20, forms an H bond (2.8 Å), and thus moves closer to the mutated residue (4.9 Å). Wat = water molecule.



Scheme 2. Comparison of the GROMOS scheme and our modified one (bold) for the description of the O3 end of progesterone: effective atomic charges and percent hydrogen bonds formed during MD simulations (2 ns each) with the two force fields.

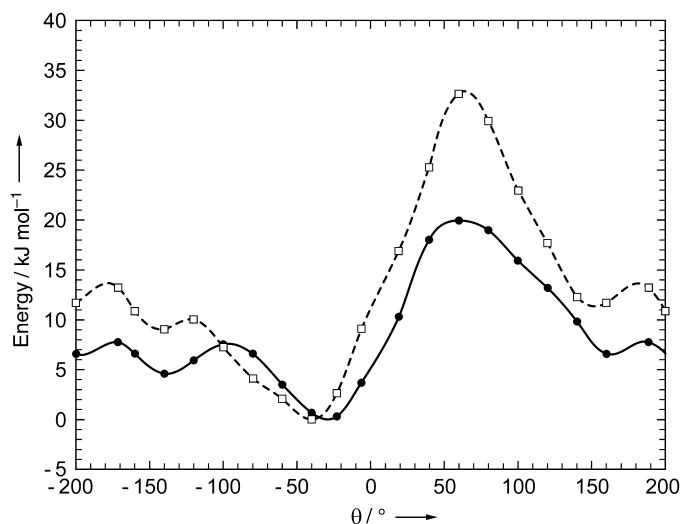


Figure 2. Energy profile of progesterone versus the torsional angle θ (C16-C17-C20-O20): *ab initio* (solid line) compared with GROMOS (dashed line) values.

solvent. This is particularly true for Arg766, which fails to act as the main bonding partner of progesterone in simulations based on the GROMOS charges. In our modified scheme for the charge distribution, the interaction between O3 and Arg766 stabilizes itself, in agreement with experimental data and chemical intuition.

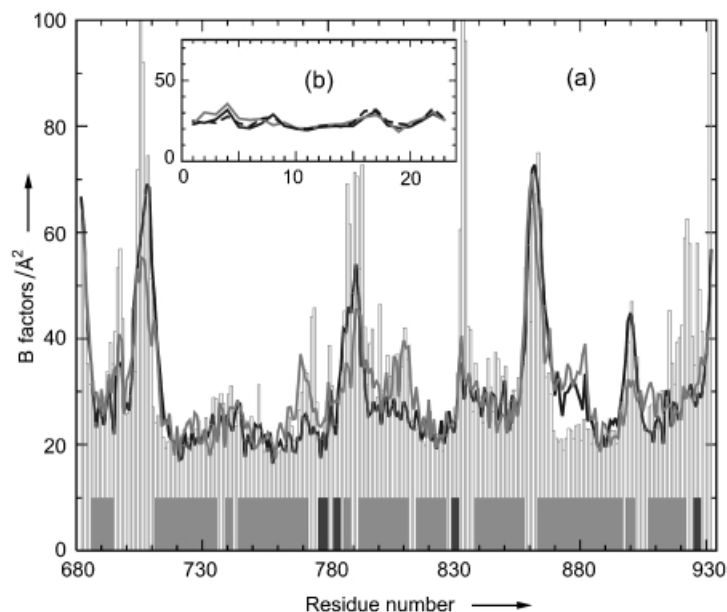


Figure 3. Debye–Waller or B factors of (a) the protein and (b) progesterone: theory versus experiment. The two different experimental curves (solid lines) refer to the two chains of the dimer. The computed values are represented by a histogram in (a) and by a dashed line in (b). Note that the side chains of residues 704–707 (located in an outer loop) were missing in the refinement of the X-ray data and thus modeling of the initial configuration was required. Gray and black squares indicate α helices and β sheets, respectively. The flexibility of some residues in the simulations (loops and C terminus) is enhanced by both the absence of the crystal environment and the presence of bulk solvent.

The results above give us confidence in approaching the thorny issue of the role of the O20 end of the hormone in binding. The X-ray refinement (Figure 1 b) could not identify any H bond partner for progesterone among the possible candidate residues, namely, Cys891, Thr894, and Asn719. Our simulations reveal a clear scenario (Figure 1 d), in which Thr894 is by far the most probable binding partner, whereas Cys891 binds to the ligand only sporadically, and Asn719 is permanently too far away. One water molecule easily diffuses into the binding pocket and is trapped there, where it stabilizes the complex by exchanging hydrogen bonds with each of the three residues mentioned and the ligand. This effect is clearly evidenced by the electron localization function (ELF)^[17] plot in Figure 4 a. Thr894 appears to be especially flexible and switches within about 2 ns between two different orientations, with a probability ratio of 2:3 between that observed in the X-ray structure and the other orientation. This rotation, however, does not alter the distance of Thr894 from O20 significantly. This distance is 0.5–0.7 Å lower than the value obtained from the X-ray refinement (Figure 1 d). The O20 end rotates only rarely. Over the 2-ns trajectory, the probability of forming H bonds between Thr894 and O20 is approximately 50%.

Other distances in the LBD also exhibit significant discrepancy between the simulation and the crystal phase. We note however that no water molecule was detected in the proximity of O20 by X-ray diffraction, in clear contrast to observations made in the simulations of the system in solution. To understand the significance of this discrepancy, we performed further simulations: Starting from the same initial configurations as those just discussed, we restrained the position of the particular water

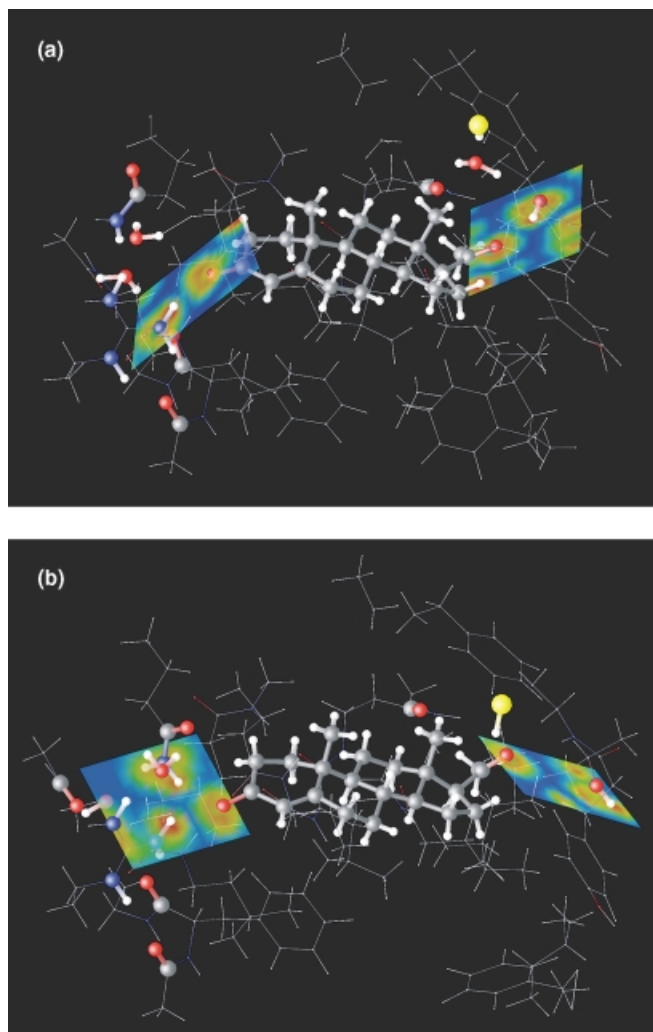


Figure 4. Electron localization function around the two polar ends of progesterone in aqueous solution: (a) the binding configuration of Thr894 with O20; (b) the configuration in the absence of the bridging water molecule in the proximity of O20, which corresponds to the X-ray structure. Note that high (low) values of the ELF shown in red (blue) denote regions of charge accumulation (depletion).

molecule we observed to easily diffuse into the complex; this water molecule was kept outside the binding pocket (the average oxygen–acetyl-group separation over the entire simulation amounted to 13 Å). Throughout the subsequent MD run, no water molecule diffused into the binding pocket. This indicates that, in contrast to the case of the O3 binding region, where water diffusion happens easily, at the O20 end the existence of an energy barrier renders access by water more difficult. Thr894 continued to be the primary binding partner for O20, but only in one of its conformations. When the same orientation as in the crystal structure was assumed for Thr894, formation of H bonds with O20 was no longer observed. This result can easily be deduced from the ELF distribution in Figure 4b. Moreover, in this case all distances are in close agreement with experimental evidence (Figure 1 f). The absence of the water molecule around the O20 end does not affect the interactions at the O3 end in any significant way (Figure 1 e).

Therefore, we can now conclude that the puzzle that emerges from the X-ray study results from the predominance of configurations in which both the torsional degrees of freedom of Thr894 are “frozen in” and no water molecule is trapped in the binding pocket of O20. This situation is not unreasonable in a crystal phase in which the degrees of freedom of the system are certainly reduced with respect to those available in solution. One can also speculate that the access of water molecules to the binding pocket may well depend on the crystallization procedure. In principle, one could also argue that the analysis of the electron density observed at the O20 region was not sufficiently accurate to reveal the presence of a water molecule. It would be interesting to check this hypothesis. Nuclear magnetic resonance spectroscopy could help further clarify this issue.

On the basis of our results, we can now rationalize the outcome of the investigations made with site-directed mutagenesis.^[2] Although our method does not allow us to calculate activation rates with the required accuracy, we can nevertheless obtain insights into the mechanisms that determine loss of activity through the identification of bonding partners and direct observation of the temporal evolution of the different systems.

The fact that mutations of both Arg766 and Gln725 cause the binding activity to vanish^[2] is consistent with both X-ray data and our findings with regard to the primary partners of O3.^[18] The effects of mutations at the O20 end of the hormone, on the other hand, are less straightforward to interpret. The binding activity is strongly reduced^[2] when Thr894 is replaced by Val (dissociation constant, K_d , varies from 6.2 nM for the wild type to 10.4 nM for the Thr894Val mutant) and vanishes when Cys891 is substituted with Ser. The former effect can be rationalized as a direct outcome of the loss of the primary binding pattern of O20, but the latter observation cannot be explained in these terms. Contrary to previous suggestions,^[2] our simulations tend to exclude the possibility that Cys891 is directly involved in the bonding. Experimental data call for a more specific investigation. To this end, we performed a series of analogous simulations of the complex with Cys891 replaced by Ser, and also of the receptor and its mutant in the absence of progesterone. No significant change was observed at the O3 end, but the effect at the O20 end is dramatic. The enhanced hydrophilic character of Ser lowers the barrier for the penetration of water into the binding pocket. In particular, simulations of the bare mutated receptor in aqueous solution reveal the formation of a cluster of water molecules, which is also stabilized by the interaction with Thr894. We observe no water clustering in analogous simulations of the wild-type progesterone receptor. Therefore, we propose that this cluster could act as an inhibiting factor in the binding process of progesterone to the mutated receptor, and increase the desolvation energy. Although long-range interactions may also play a role in the observed loss of binding activity, the phenomenon we have discovered is realistic and might well contribute to this loss.

The study presented above provides a solution to the long-standing puzzle of progesterone binding and sheds light on the results of mutation analyses. This outcome has been possible thanks to the accuracy and robustness of the computational

scheme and to the combination of high-quality X-ray structural data and MD simulations in aqueous solution. DFT-based calculations combined with suitable consistency restraints allowed reliable parametrization of the ligand. This latter step was crucial for the validity of the model of the ligand–protein complex. We believe that this multiple approach can offer an efficient procedure for the unraveling of ligand–protein binding and drug design whenever the chemical features of the ligand are misrepresented by conventional force fields. Our results are evidence of the dynamic nature of ligand–protein binding and also signal a warning about the use of conventional or inconsistently modified force fields. Therefore, other steroid/nuclear receptor LBDs might have to be reconsidered,^[19–21] even when structural data are not as puzzling as in the case of progesterone.

Methods Section

MD simulations were carried out with the GROMOS96 code by using the GROMOS force field parametrization (version 43A1)^[10] for the receptor and the SPC model^[22] for the explicit water molecules. The system consisted of progesterone (23 atoms), the receptor LBD (2586 atoms), and 10736 explicit water molecules. After the initial energy minimization, the system was equilibrated by performing a 10-ps MD simulation at constant volume with position constraints for the solute, followed by 10 ps at constant pressure. Afterwards, the solute was allowed to move freely, and the temperature was slowly raised from 50 K to 300 K, in intervals of 5-ps simulations. When the temperature had reached 300 K, a further 30-ps MD run at constant temperature and pressure was carried out. After this equilibration phase, the production run was started. This equilibration process corrects the gross problems found in the initial structure.^[5] For each system considered, the total production simulation times ranged between 2 and 2.7 ns. The entire procedure was carried out for each series of simulations. Periodic boundary conditions were applied. Nonbonded interactions were evaluated by using the twin-range cut-off method. Electrostatic interactions beyond 1.4 nm were approximated with a Poisson–Boltzmann generalized reaction field term.

Ab initio calculations^[23] were based on DFT^[12] with gradient-corrected functionals (BLYP; Becke approximation for the exchange;^[24] Lee–Yang–Parr approximation for the correlation^[25]).

The GROMOS96 effective charges for the conjugated keto group at the O3 end of the ligand were replaced by those obtained from best fitting of the ab initio electrostatic potential and restrained to the GROMOS96 range of values.^[10] We applied the fitting procedure developed by Kollman's group^[26] and conveniently modified it to include both a loose set of parabolic restraints and a stiff set. The latter set kept the charges of the chemical groups for which a specific parametrization was available in the GROMOS force field essentially unchanged, whereas the former set allowed the charge to reorganize in the O3 region without perturbing the internal Coulomb–van der Waals consistency of the force field in an uncontrolled fashion.

We also performed DFT–BLYP calculations to provide the reference energy profile to which we fitted the new torsional potential at the O20 end, as explained in the text. We verified that the positions of the minima were fully consistent with the values observed in crystal structures, circular dichroism, infrared, and nuclear magnetic reso-

nance solution spectra of pregnanes with a keto substituent at C20.^[27]

Further details of the calculations: Bond lengths for the bonds involving hydrogen atoms were constrained by the SHAKE algorithm with a relative tolerance of 10^{-4} ; MD runs were at constant (room) temperature and constant pressure; runs used a 1-fs time step; a 1-ns simulation took 14 days on a 2-processor Linux node. We calculated the electronic structure of a few configurations (around 450 atoms in the quantum subsystem) and derived the ELF^[17] with a newly developed quantum–classical scheme (CPMD/GROMOS).^[6]

We are grateful to Professor Wilfred F. van Gunsteren for his critical reading of the manuscript and his valuable suggestions for improvement. We also wish to thank the referees of our manuscript for their constructive suggestions.

- [1] S. P. Williams, P. B. Sigler, *Nature* **1998**, *393*, 392–396.
- [2] M. Letz, P. Bringmann, M. Mann, A. Mueller-Fahrnow, D. Reipert, P. Scholz, J.-M. Wurtz, U. Egner, *Biochim. Biophys. Acta* **1999**, *1429*, 391–400.
- [3] R. V. Weatherman, R. J. Fletterick, T. S. Scanlan, *Annu. Rev. Biochem.* **1999**, *68*, 559–581, and references therein.
- [4] J. P. Renaud, D. Moras, *Cell. Mol. Life Sci.* **2000**, *57*, 1748–1769, and references therein.
- [5] Gross problems in the structure 1a28.pdb described by the WHAT CHECK report (www.cmbi.kun.nl/gv/pdbreport/) regard residues either on the external loops or on the surface, which are far away from the binding site of progesterone.
- [6] W. Andreoni, A. Curioni, T. Mordasini, *IBM J. Res. Dev.* **2001**, *45*, 397–407, and references therein.
- [7] According to the philosophy of this work, the quantum subsystem of minimum size would be progesterone, which contains 53 atoms. We estimate that a 1-ns run would require 100 days on an IBM p690 server with 32 Power4 processors (160 Gflop peak).
- [8] J.-Y. Le Questel, G. Boquet, M. Berthelot, C. Laurence, *J. Phys. Chem. B* **2000**, *104*, 11 816–11 823.
- [9] B. C. Oostenbrink, J. W. Pitera, M. M. H. van Lipzig, J. H. N. Meerman, W. F. van Gunsteren *J. Med. Chem.* **2000**, *43*, 4594–4605.
- [10] W. F. van Gunsteren, S. R. Billeter, A. A. Eising, P. H. Hünenberger, P. Krüger, A. E. Mark, W. R. P. Scott, I. G. Tironi, *Biomolecular Simulation: The GROMOS96 Manual and User Guide*, VdF: Hochschulverlag AG der ETH Zürich, Zurich, Switzerland, and BIOMOS b.v., Groningen, The Netherlands, **1996**, ISBN 37281 2422 2.
- [11] W. R. P. Scott, P. H. Hünenberger, I. G. Tironi, A. E. Mark, S. R. Billeter, J. Fennen, A. E. Torda, T. Huber, P. Krüger, W. F. van Gunsteren, *J. Phys. Chem. A* **1999**, *103*, 3596–3607.
- [12] See, for example, R. M. Dreizler, E. K. U. Gross, *Density Functional Theory*, Springer-Verlag, Berlin, **1990**.
- [13] D. M. Tanenbaum, Y. Wang, S. P. Williams, P. B. Sigler, *Proc. Natl. Acad. Sci. U.S.A.* **1998**, *95*, 5998–6003.
- [14] T. A. Halgren, *J. Comput. Chem.* **1999**, *20*, 730–748, and references therein.
- [15] C. A. Marhefka, B. M. Moore II, T. C. Bishop, L. Kirkovsky, A. Mukherjee, J. T. Dalton, D. D. Miller, *J. Med. Chem.* **2001**, *44*, 1729–1740.
- [16] P. H. Hünenberger, A. E. Mark, W. F. van Gunsteren, *J. Mol. Biol.* **1995**, *252*, 492–503.
- [17] J. K. Burdett, T. A. McCormick, *J. Phys. Chem. A* **1998**, *102*, 6366–6372.
- [18] Mutations at O3 are expected to have a more dramatic effect than those at O20 on the basis of the predominant role of O3 in stereoidic recognition (see, for example, R. Bursi, M. B. Groen, *Eur. J. Med. Chem.* **2000**, *35*, 787–796).
- [19] R. L. Wagner, J. W. Apriletti, M. E. McGrath, B. L. West, J. D. Baxter, R. J. Fletterick, *Nature* **1995**, *378*, 690–697.
- [20] A. M. Brzozowski, A. C. W. Pike, Z. Dauter, R. E. Hubbard, T. Bonn, O. Engström, L. Öhman, G. L. Greene, J.-A. Gustafsson, M. Carlquist, *Nature* **1997**, *389*, 753–758.
- [21] P. M. Matias, P. Donner, R. Coelho, M. Thomaz, C. Peixoto, S. Macedo, N. Otto, S. Joschko, P. Scholz, A. Wegg, S. Bäsler, M. Schäfer, U. Egner, M. A. Carrondo, *J. Biol. Chem.* **2000**, *275*, 26164–26171.

- [22] H. J. C. Berendsen, J. P. M. Postma, W. F. van Gunsteren, J. Hermans in *Intermolecular Forces* (Ed.: B. Pullman), Reidel, Dordrecht, The Netherlands, **1981**, pp. 331 – 342.
- [23] We used the CPMD code (Copyright IBM Corporation **1990** – **1997** and MPI Festkörperforschung, Stuttgart, Germany, **1997**; www.cpmd.org), which is based on a plane-wave expansion of the electron wavefunction and on atomic pseudopotentials.
- [24] A. D. Becke, *Phys. Rev.* **1988**, *38*, 3098 – 3100.
- [25] C. Lee, W. Yang, R. G. Parr, *Phys. Rev.* **1988**, *37*, 785 – 789.
- [26] C. I. Bayly, P. Cieplak, W. D. Cornell, P. A. Kollman, *J. Phys Chem.* **1993**, *97*, 10269 – 10280.
- [27] W. L. Duax, J. F. Griffin, D. C. Rohrer, *J. Am. Chem. Soc.* **1981**, *103*, 6705 – 6712, and references therein.

Received: July 1, 2002

Revised version: November 26, 2002 [F 445]